

An Iron–Sulfur Cluster in the Polymerase Domain of Yeast DNA Polymerase ϵ

Rinku Jain¹, Eva S. Vanamee¹, Boris G. Dzikovski², Angeliki Buku¹, Robert E. Johnson³, Louise Prakash³, Satya Prakash³ and Aneel K. Aggarwal¹

1 - Department of Structural and Chemical Biology, Mount Sinai School of Medicine, Box 1677, 1425 Madison Avenue, New York, NY 10029, USA

2 - Department of Chemistry and Chemical Biology, Cornell University, Ithaca, NY 14853, USA

3 - Department of Biochemistry and Molecular Biology, University of Texas Medical Branch, 301 University Boulevard, Galveston, TX 77755-1061, USA

Correspondence to Aneel K. Aggarwal: Fax: +1 212 849 2456. Aneel.Aggarwal@mssm.edu
<http://dx.doi.org/10.1016/j.jmb.2013.10.015>

Edited by J. Berger

Abstract

DNA polymerase ϵ (Pol ϵ) is a multi-subunit polymerase that contributes to genomic stability via its roles in leading strand replication and the repair of damaged DNA. Pol ϵ from *Saccharomyces cerevisiae* is composed of four subunits—Pol2, Dpb2, Dpb3, and Dpb4. Here, we report the presence of a [Fe-S] cluster directly within the active polymerase domain of Pol2 (residues 1–1187). We show that binding of the [Fe-S] cluster is mediated by cysteines in an insertion (Pol2^{ins}) that is conserved in Pol2 orthologs but is absent in the polymerase domains of Pol α , Pol δ , and Pol ζ . We also show that the [Fe-S] cluster is required for Pol2 polymerase activity but not for its exonuclease activity. Collectively, our work suggests that Pol ϵ is perhaps more sensitive than other DNA polymerases to changes in oxidative stress in eukaryotic cells.

© 2013 Elsevier Ltd. All rights reserved.

The survival of all organisms depends on the ability to faithfully replicate the genome. In eukaryotes, with genomes ranging in size from millions to billions of base pairs, the bulk of DNA synthesis is carried out by three polymerases [1,2]: Pol α , Pol δ , and Pol ϵ . Pol α primes the Okazaki fragments on the lagging strand, which are then elongated by Pol δ . Pol ϵ is believed to be the leading strand polymerase and, like Pol δ , achieves fidelity via both accurate DNA polymerization and 3' → 5' proofreading exonuclease activities. Pol α , Pol δ , and Pol ϵ belong to the B-family of DNA polymerases and are conserved in all eukaryotes. Eukaryotes also possess a lower fidelity B-family polymerase, Pol ζ , which promotes synthesis through DNA lesions that block replication [3].

The *Saccharomyces cerevisiae* Pol α (Pol1, Pol12, Pri1, Pri2), Pol ϵ (Pol2, Dpb2, Dpb3, Dpb4), Pol δ (Pol3, Pol31, Pol32), and Pol ζ (Rev3, Rev7, Pol31, Pol32) are multi-subunit polymerases with catalytic and regulatory subunits [1,2,4]. The catalytic subunits Pol1, Pol2, Pol3, and Rev3 are modular with a large N-terminal exonuclease–polymerase (exo–pol) catalytic core

followed by a small metal binding domain at the C-terminus (CTD; Fig. 1a). In Pol2, an additional inactive exo–pol module is observed between the N-terminus active exo–pol module and the CTD [5]. Recent studies on eukaryotic B-family Pols have established the presence of a [4Fe-4S] cluster in the CTDs of Pol3 and Rev3 [6–8]; though for the Pol1 and Pol2 CTDs, there is some degree of uncertainty [6,8]. An [Fe-S] cluster has also been found in the Pri2 subunit of Pol α [9–11]. Taken together, the observation of Fe-S clusters in eukaryotic DNA polymerases is part of emerging evidence on their importance in essential components of the nucleic acid processing machineries [12]. We show here that Pol ϵ contains a [Fe-S] cluster directly within its first active exo–pol catalytic core and that this [Fe-S] cluster is necessary for its polymerase activity.

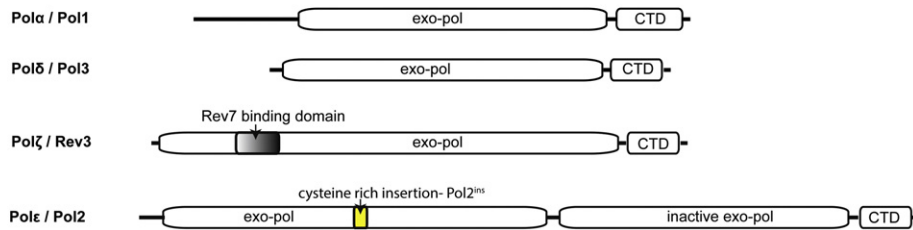
The first clue that the Pol ϵ catalytic core contained a [Fe-S] cluster came during protein purification. We observed that samples of Pol2 containing only the exo–pol catalytic core (Pol2 Δ CTD; residues 1–1187), purified from yeast or *Escherichia coli* cells,

were yellowish-brown in color (Fig. 1b) and that the color was concentration dependent. UV-Vis spectrum of Pol2 Δ CTD exhibited a broad maxima centered at \sim 400 nm (Fig. 1c), suggesting the presence of a [Fe-S] cluster. Biochemical analysis with an iron-specific indicator (bathophenanthroline), which turned pink in the presence of Pol2 Δ CTD but not a control buffer, also suggested the presence of non-heme iron in Pol2 Δ CTD. The assay yielded a stoichiometric molar ratio of 2:1 iron:protein for the *E. coli* expressed Pol2 Δ CTD.

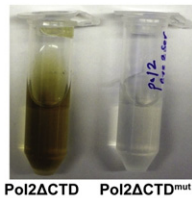
Next, we analyzed the Fe-S cluster in Pol2 Δ CTD by extended X-ray absorption fine structure (EXAFS) spectroscopy, using synchrotron radiation at Brookhaven National Laboratory (beamline X3B). EXAFS is a powerful technique for characterizing an element and its coordination in a protein sample [13]. The

EXAFS data clearly showed the presence of Fe in Pol2 Δ CTD. Figure 2a shows the Fourier transform EXAFS (FT-EXAFS) data and the best fit. The first shell peak in the FT-EXAFS data corresponds to Fe-S backscattering, and the second shell peak is the result of Fe-Fe backscattering. Subsequent scans showed a reduction in the size of the Fe-Fe peak, which indicates oxidation. For this reason, we used only the first scan of each spot, merging a total of three scans for data analysis. The data can be best fit to a [4Fe-4S] cluster with an Fe-S distance of 2.29 Å and a Fe-Fe distance of 2.72 Å. The fitting data are summarized in Supplementary Table 1. The fitting results are similar to those obtained for other [4Fe-4S] clusters with a reduced iron center [18]. Fits to a [2Fe-2S] cluster gave consistently worse results, though the presence of a [2Fe-2S] cluster cannot

(a) Domain organization in the catalytic subunit of eukaryotic B-Family polymerases



(b) Purified Pol2



(c) UV-vis absorption spectra

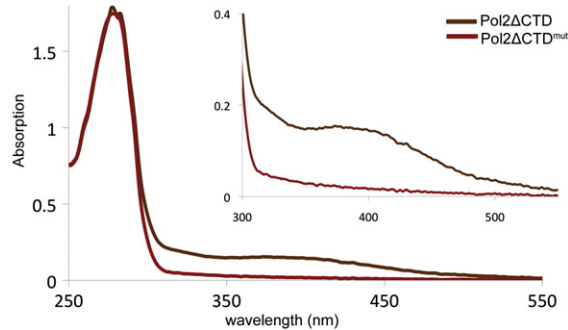


Fig. 1. Catalytic subunits of eukaryotic B-family polymerase and characterization of Pol2 variants. (a) Domain organization in the catalytic subunit of eukaryotic B-family polymerases. In each case, an N-terminal exonuclease-polymerase (exo-pol) domain is followed by a metal binding C-terminal domain (CTD). Pol2 has an inactive exo-pol module between its active N-terminal exo-pol domain and the CTD. Approximate location of the cysteine-rich motif within the polymerase domain of Pol2 is indicated in yellow. (b) Purified Pol2 Δ CTD is yellowish-brown in color while Pol2 Δ CTD^{mut} is colorless at the same concentration. The *S. cerevisiae* Pol2 Δ CTD and Pol2 Δ CTD^{mut} were expressed in yeast strain YRP654 (MAT α ura3-52 trp1 Δ leu2 Δ 1 his3- Δ 200 pep4::HIS3 prb1 Δ 1.6R can1 GAL) by induction with 2% galactose for 18 h. Both proteins were purified by affinity chromatography on glutathione Sepharose 4B beads, removal of the glutathione S-transferase tag by cleavage with PreScission protease, and further purification by size exclusion on a Superdex 200 column (GE Healthcare). For purification from *E. coli* cells, yeast Pol2 Δ CTD and Pol2 Δ CTD^{mut} were expressed with a His₆ tag at the N-terminus and purified by affinity chromatography on a Ni-NTA agarose column (Qiagen), followed by ion exchange (HiTrapQ; GE Healthcare) or affinity chromatography on a Heparin column and size-exclusion (Superdex 200; GE Healthcare) chromatography. (c) UV-Vis absorption spectra of Pol2 Δ CTD and Pol2 Δ CTD^{mut}. Inset shows the broad shoulder centered at 400 nm that is characteristic of Fe-S cluster in the Pol2 Δ CTD spectrum and missing in the spectrum of Pol2 Δ CTD^{mut}. UV-Vis spectra were recorded under aerobic conditions at room temperature on a Nanodrop 2000c Spectrophotometer (Thermo Scientific).

entirely be ruled out based on the EXAFS data alone.

EPR analysis on Pol2 Δ CTD [19] also suggested the presence of [Fe-S] cluster (Fig. 2b). The EPR signal of purified Pol2 Δ CTD increased considerably upon reduction with sodium dithionite. The dominant g -values of 1.98 and 2.023 observed in the EPR spectrum are consistent with the presence of either [4Fe-4S] or [2Fe-2S] cluster in Pol2 Δ CTD (Fig. 2b). The spectrum was best observed at 12 K, as the intensity decreased with increasing temperature and disappeared completely at 35 K. The temperature dependence of the Pol2 Δ CTD EPR spectrum is characteristic of [Fe-S] clusters, [4Fe-4S] in particular.

We further confirmed the presence of iron in Pol2 Δ CTD by inductively coupled plasma (ICP) emission. ICP analysis indicated the presence of 2.4 moles of iron per mole of protein and no significant amounts of zinc, cobalt, nickel, manganese, and magnesium (Table 1). The stoichiometry of less than 4 observed by ICP for Pol2 Δ CTD has also been observed previously for other [4Fe-4S] proteins [11,20] and can be attributed to loss of iron during aerobic purification and concentration. Together, our biochemical, EXAFS, EPR, and ICP analyses provide strong evidence for the existence of a [Fe-S] cluster in the first active polymerase domain of Pol2.

Pol2 is phylogenetically related to Pol1, Pol3, and Rev3, which belong to the B-family of DNA polymerases (Fig. 3a). Despite this homology, samples of Pol1 Δ CTD, Pol3 Δ CTD, and Rev3 Δ CTD purified over the years in our laboratory are colorless (data not shown), suggesting that the Fe-S cluster binding is specific to the polymerase domain of Pol2. To identify putative metal binding features in Pol2 Δ CTD that are absent from the other homologs, we undertook primary sequence alignment of the catalytic subunits of eukaryotic B-family polymerases. Sequence alignment revealed a cysteine-rich insertion (Pol2^{ins}) between motif A (in the palm domain) and motif B (in the fingers domain) that is conserved in Pol2 from different species (Fig. 3b) but is absent in Pol1, Pol3, and Rev3. Computational analysis with MetalDetector [22] for predicting metal binding sites suggested four cysteines in the *S. cerevisiae* Pol2 Δ CTD (Cys665, Cys668, Cys677, and Cys763) as putative metal binding ligands. To test this prediction, we generated a Pol2 Δ CTD mutant with three of the putative Fe-S ligands (Cys665, Cys668, and Cys677) mutated to serine. Compared to the wild-type Pol2 Δ CTD, the Pol2 Δ CTD triple mutant (Pol2 Δ CTD^{mut}) was colorless (Fig. 1b) and its UV-Vis spectrum lacked the broad peak centered at 400 nm (Fig. 1c) that is indicative of a [Fe-S] cluster. Moreover, no significant metal content was detected by ICP analysis of Pol2 Δ CTD^{mut} at the same concentration as the wild-type protein (Table 1). Together, these observations suggest

that cysteine residues in Pol2^{ins} are involved in [Fe-S] cluster binding, and mutations to serine result in impaired cluster incorporation. Also, the mutant had a slightly higher tendency to aggregate than the wild-type protein, suggesting a role for the [Fe-S] cluster in Pol2 folding.

To further examine the role of [Fe-S] cluster in Pol2 Δ CTD folding and enzymatic activity, we tested both the wild type and the mutant protein for their ability to synthesize primers on a primer-template duplex (Fig. 3d). As expected, Pol2 Δ CTD was catalytically efficient and able to insert nucleotide and extend the primer. In contrast to the wild-type Pol2 Δ CTD, Pol2 Δ CTD^{mut} was significantly deficient in DNA synthesis activity and unable to extend the primer to the end of the template strand (Fig. 3d). However, it exhibited a slightly higher exonuclease activity, presumably due to the absence of any DNA synthesis activity. These results suggest that the [Fe-S] cluster is important for the DNA synthesis activity of Pol2 but has no effect on its exonuclease activity.

Fe-S clusters are ancient cofactors associated most commonly with enzymes that mediate electron transfer during energy conversion [23,24]. Surprisingly, [Fe-S] clusters have also now been identified in nucleic acid processing enzymes such as glycosylases, helicases, and polymerases, which have no obvious roles in electron transfer [12]. The [Fe-S] clusters appear to play a structural role in these enzymes, though there is evidence that some of these enzymes also use the redox properties of the Fe-S cluster to execute DNA transactions, from binding and unwinding to the sensing of lesions [12]. The [4Fe-4S] cluster in the CTD of eukaryotic Pol δ and Pol ζ helps to maintain the structural integrity of the second metal binding motif (CysB) for interactions with the regulatory B-subunit (Pol31) [6–8]. In Pol α and Pol ϵ , the situation is more complex, with evidence for the presence of Fe or Zn in the CysB of their CTDs [6,8,25]. We show here that Pol ϵ contains an Fe-S cluster directly within its active N-terminal exo-pol catalytic core. The Fe-S cluster is coordinated by cysteines on an “insertion” that is conserved in Pol2 orthologs but is absent from the catalytic subunits of Pol α , Pol δ , and Pol ζ .

Although a crystal structure of the Pol2 catalytic core remains to be determined, a reasonable model can be constructed based on the crystal structure of the Pol3 catalytic domain [21], composed of palm, fingers, thumb, and N-terminal domains for polymerase activity and an exonuclease domain for proofreading activity (Fig. 3a). From our model, the Fe-S cluster in Pol2 maps to the “hinge” between the palm and fingers domain, not too far from the polymerase active site to have a direct effect on its polymerization activity (Fig. 3c). Interestingly, the [Fe-S] cluster is on the opposite side of the catalytic core as the exonuclease domain (> 60 Å away), which may explain why the loss

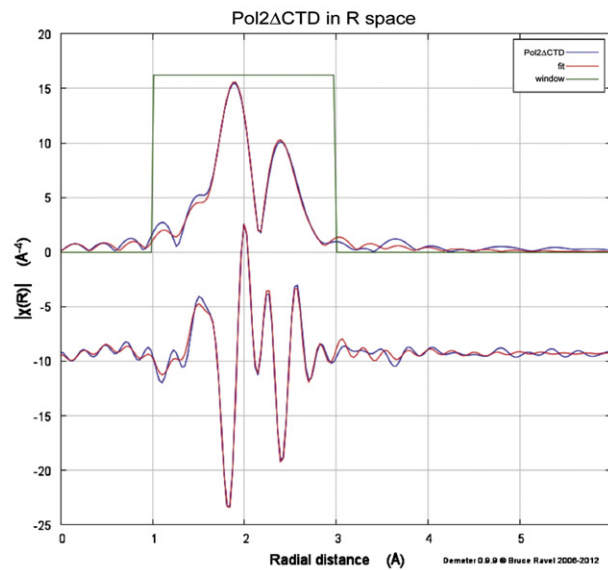
of cluster binding correlates with loss of polymerase activity but has no effect on the exonuclease activity (Fig. 3d).

Fe-S clusters do not assemble spontaneously but require a set of proteins in the mitochondria [26]. After synthesis in the mitochondria, some of the [Fe-S] clusters are exported to the cytoplasm, where the MMS19 protein has recently been shown to be part of the complex that transfers [Fe-S] clusters to target proteins [27,28]. Defects in both mitochondria and MMS19 have been directly linked to nuclear genomic instability [27–29], and based on our results, a significant portion of this instability may arise from the loss of the [Fe-S] cluster in the Pol ϵ catalytic core. Pol ϵ contributes to genomic stability via its role not only in leading strand replication but also in the repair of damaged DNA [30]. We show here that an [Fe-S] cluster stabilizes the catalytic core of Pol ϵ for DNA synthesis. Also, the relatively solvent-exposed position of the [Fe-S] cluster in the

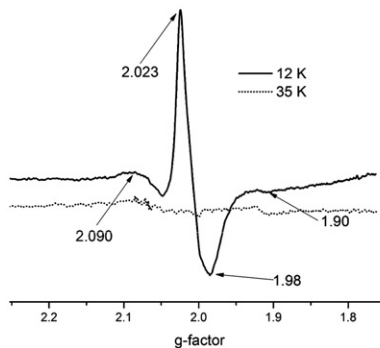
hinge between the palm and fingers domain may allow for interactions with other components of the eukaryotic replication machinery. Importantly, the sensitivity of the [Fe-S] cluster to oxidation may provide a means to couple DNA synthesis and repair by Pol ϵ to oxidative stress in eukaryotic cells.

In conclusion, the finding of a [Fe-S] cluster in the catalytic core of Pol2 changes our view of Pol ϵ . It suggests a polymerase that is perhaps more sensitive than others to mitochondrial dysfunction, defects in [Fe-S] biogenesis, and changes in oxidative stress in eukaryotic cells. Altogether, the [Fe-S] cluster in Pol2 adds to the growing evidence on the importance of [Fe-S] clusters in nucleic acid processing machineries and provides a new impetus for experiments on the correlation between DNA metabolism and the redox environment of a cell.

(a) FT-EXAFS data of Pol2 Δ CTD



(b) EPR spectra of Pol2 Δ CTD



Acknowledgements

We thank the staff at Brookhaven National Laboratory (beamline X3B) for help with EXAFS data collection. The work was partially supported by grants CA138546 and CA107650 from the U.S. National Institutes of Health. The EPR studies were supported by National Institutes of Health grant P41GM103521.

Appendix A. Supplementary data

Supplementary data to this article can be found online at <http://dx.doi.org/10.1016/j.jmb.2013.10.015>

Received 6 September 2013;

Accepted 8 October 2013

Available online 19 October 2013

Keywords:

DNA replication;
DNA polymerase;
DNA repair;
Fe-S cluster;
oxidative stress

Table 1. Element concentration by ICP emission spectroscopy

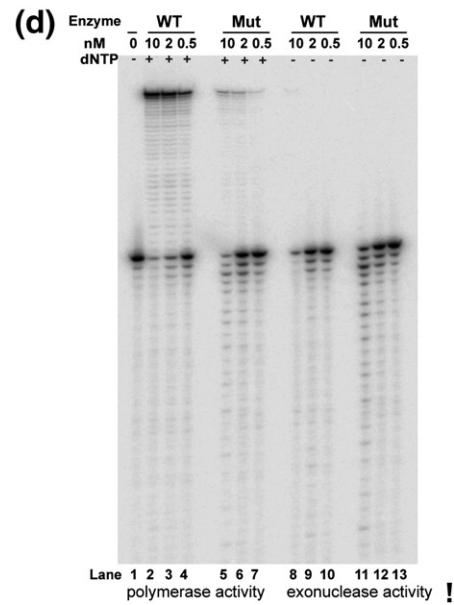
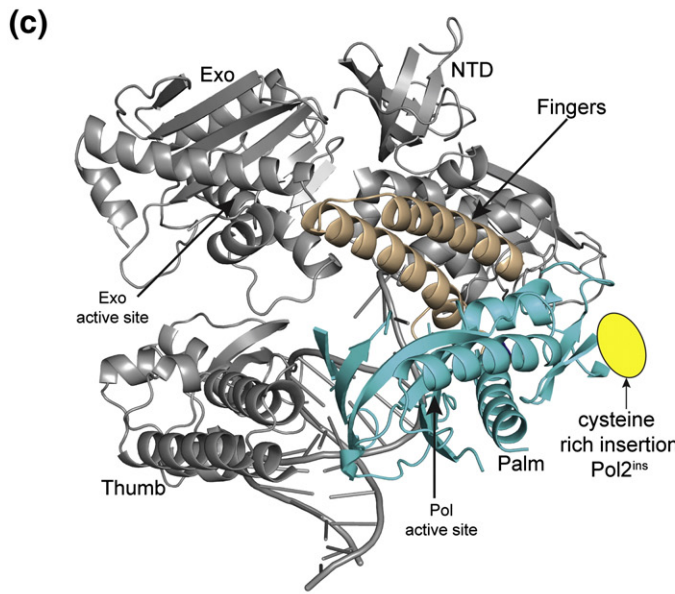
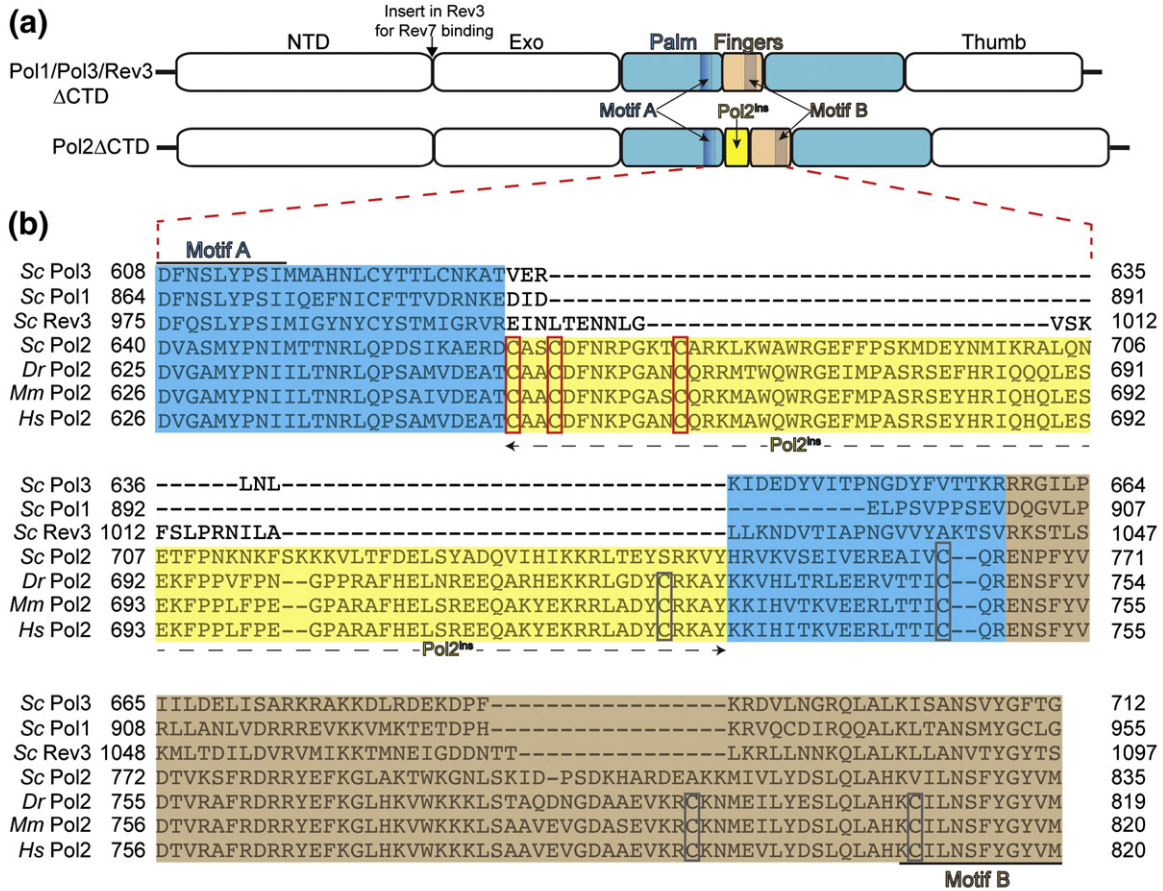
Element	[Fe]:[protein] Pol2 Δ CTD	[Fe]:[protein] Pol2 Δ CTD ^{mut}
Ca	0.03	0.04
Co	—	0.00
Cu	0.02	0.01
Fe	2.35	0.01
Mg	0.01	0.00
Mn	0.00	0.00
Mo	—	—
Ni	0.03	0.13
Zn	0.07	0.06

Metal content of Pol2 Δ CTD and Pol2 Δ CTD^{mut} was determined by ICP at the University of Georgia Chemical Analysis Laboratory. Proteins were concentrated to 16 mg/ml in buffer containing 25 mM Tris-HCl (pH 8.0), 2 mM tris(2-carboxyethyl)phosphine, 5% glycerol, and 400 mM NaCl, and the filtrate from the concentration step was used as a blank. The concentrations of 20 different elements were determined simultaneously. Ratios for some metals that are commonly found in metalloenzymes are shown.

Abbreviations used:

EXAFS, extended X-ray absorption fine structure;
FT-EXAFS, Fourier transform EXAFS; ICP, inductively coupled plasma.

Fig. 2. Spectroscopic analysis of Pol2 Δ CTD. (a) The FT-EXAFS data of Pol2 Δ CTD (blue line) superimposed on the best fit (red line). Pol2 Δ CTD samples were concentrated to a final concentration of 370 μ M as judged by absorbance at 280 nm. The samples were loaded into a 0.5-mm-thick copper sample holder containing three 4.5 mm \times 12 mm holes that were sealed on one side with an Fe-free Kapton tape. Each hole was filled with \sim 50 μ l of sample. Fe K-edge X-ray absorption spectroscopic data were collected at the National Synchrotron Light Source on beamline X3B. The beamline is equipped with a sagittally focused Si(111) double crystal monochromator. A Ni mirror at an angle of 4.5 mrad was used to reject higher-order harmonic contamination. All experiments were carried out at 15 K in a closed cycle He cryostat under vacuum. EXAFS data were collected with 0.05 \AA^{-1} step sizes in k space starting at 25 eV photoelectron energy. The signal averaging was weighted with respect to k so that 2 s per point was used at $k = 1$ and 7 s per point was used at $k = 15$. Below 25 eV, data were collected by counting at a specific energy for 1 s and incrementing the energy by 10 eV from 200 eV below the iron edge to 10 eV below the edge, then in 0.3 eV steps up to 25 eV above the edge with 1 s per point signal averaging. To reduce the possibility of sample degradation, the X-ray beam was moved on the sample holder, and 3–5 scans were collected on each of the three different sample holes. Data were taken in the range 180- to 300-mA beam current. Fe K- α fluorescence was detected at 90° angle from the incident beam using a 31-element, energy-resolving Ge detector [14]. The internal count rates were kept at or less than 30,000/s per channel to avoid saturation effects in the detector. A calibration channel behind the sample was set up to detect the spectrum of a Fe foil simultaneously with all sample spectra. This calibration channel provided a reference for the energy calibration of the sample spectra; the K-edge inflection point assigned as 7112 eV. EXAFS data analysis was performed by the EXAFS program suite Demeter (v. 0.9.9) that contains the programs ATHENA, ARTEMIS [15,16], and FEFF on an IBM-compatible machine running under Microsoft Windows XP. Data manipulation with use of a linear pre-edge fit, cubic polynomial spline background subtraction, wavevector cubed weighting, and Fourier transformation were performed using ATHENA. The theoretical data were generated using the ab initio code FEFF (v.6) [17]. The coordinates of iron models were extracted from known crystal structures deposited in the Protein Data Bank using a 6- \AA radius around the Fe(II) ion. The first and second shell [4Fe-4S] contribution from PDB ID 1EYT and the first and second shell [2Fe-2S] contribution from PDB ID 1F37. The theoretical data were fit to the unfiltered experimental k^3 weighted χ data using the non-linear, least-squares method *sin*g iFEFFIT implemented in ARTEMIS by fixing the coordination number (N) and letting all other parameters to float. The program also performs error analysis and calculates goodness-of-fit parameters. An R window of 1–3 was used for the Fourier backtransform and fitting. (b) EPR spectra of Pol2 Δ CTD after treatment with sodium dithionite at 12 K and 35 K; g -values are indicated. For EPR spectrum acquisition, Pol2 Δ CTD purified aerobically was reduced by the addition of 10 mM sodium dithionite. Spectra were recorded on BRUKER ELEXSYS E500 EPR spectrophotometer at 9.32 GHz, microwave power of 0.63 mW, and modulation amplitude of 6G. Data were acquired from frozen glasses at 12 K or 30 K using ESR910 Oxford Instruments liquid helium cryostat. The field sweeps were calibrated with a BRUKER ER 035 Gauss meter, and the microwave frequency was monitored with a frequency counter. Data acquisition and manipulation were performed with Xep software.



References

- [1] Johnson A, O'Donnell M. Cellular DNA replicases: components and dynamics at the replication fork. *Annu Rev Biochem* 2005;74:283–315.
- [2] Johansson E, Macneill SA. The eukaryotic replicative DNA polymerases take shape. *Trends Biochem Sci* 2010;35:339–47.
- [3] Prakash S, Johnson RE, Prakash L. Eukaryotic translesion synthesis DNA polymerases: specificity of structure and function. *Annu Rev Biochem* 2005;74:317–53.
- [4] Johnson RE, Prakash L, Prakash S. Pol31 and Pol32 subunits of yeast DNA polymerase delta are also essential subunits of DNA polymerase zeta. *Proc Natl Acad Sci U S A* 2012;109:12455–60.
- [5] Tahirov TH, Makarova KS, Rogozin IB, Pavlov YI, Koonin EV. Evolution of DNA polymerases: an inactivated polymerase-exonuclease module in Pol epsilon and a chimeric origin of eukaryotic polymerases from two classes of archaeal ancestors. *Biol Direct* 2009;4:11.
- [6] Baranovskiy AG, Lada AG, Siebler HM, Zhang Y, Pavlov YI, Tahirov TH. DNA polymerase delta and zeta switch by sharing accessory subunits of DNA polymerase delta. *J Biol Chem* 2012;287:17281–7.
- [7] Makarova AV, Stodola JL, Burgers PM. A four-subunit DNA polymerase zeta complex containing Pol delta accessory subunits is essential for PCNA-mediated mutagenesis. *Nucleic Acids Res* 2012;40:11618–26.
- [8] Netz DJ, Stith CM, Stumpfig M, Kopf G, Vogel D, Genau HM, et al. Eukaryotic DNA polymerases require an iron-sulfur cluster for the formation of active complexes. *Nat Chem Biol* 2012;8:125–32.
- [9] Klinge S, Hirst J, Maman JD, Krude T, Pellegrini L. An iron-sulfur domain of the eukaryotic primase is essential for RNA primer synthesis. *Nat Struct Mol Biol* 2007;14:875–7.
- [10] Sauguet L, Klinge S, Perera RL, Maman JD, Pellegrini L. Shared active site architecture between the large subunit of eukaryotic primase and DNA photolyase. *PLoS One* 2010;5:e10083.
- [11] Weiner BE, Huang H, Dattilo BM, Nilges MJ, Fanning E, Chazin WJ. An iron-sulfur cluster in the C-terminal domain of the p58 subunit of human DNA primase. *J Biol Chem* 2007;282:33444–51.
- [12] White MF, Dillingham MS. Iron-sulphur clusters in nucleic acid processing enzymes. *Curr Opin Struct Biol* 2012;22:94–100.
- [13] Strange RW, Feiters MC. Biological X-ray absorption spectroscopy (BioXAS): a valuable tool for the study of trace elements in the life sciences. *Curr Opin Struct Biol* 2008;18:609–16.
- [14] Cramer SP, Chen E, George SJ, van Elp J, Moore J, Tesch O. Soft X-ray spectroscopy of metalloproteins using fluorescence detection. *Nucl Instrum Methods Phys Res Sect A* 1992;319:289–95.
- [15] Newville M. IFEFFIT: interactive XAFS analysis and FEFF fitting. *J Synchrotron Radiat* 2001;8:322–4.
- [16] Ravel B, Newville M. ATHENA, ARTEMIS, HEPHAESTUS: data analysis for X-ray absorption spectroscopy using IFEFFIT. *J Synchrotron Radiat* 2005;12:537–41.
- [17] Rehr JJ, Mustre de Leon J, Zabinsky SI, Albers RC. Theoretical X-ray absorption fine structure standards. *J Am Chem Soc* 1991;113:5135–40.
- [18] Mitra D, George SJ, Guo Y, Kamali S, Keable S, Peters JW, et al. Characterization of [4Fe-4S] cluster vibrations and structure in nitrogenase Fe protein at three oxidation levels via combined NRVs, EXAFS, and DFT analyses. *J Am Chem Soc* 2013;135:2530–43.
- [19] Prisner T, Rohrer M, MacMillan F. Pulsed EPR spectroscopy: biological applications. *Annu Rev Phys Chem* 2001;52:279–313.
- [20] Hinks JA, Evans MC, De Miguel Y, Sartori AA, Jiricny J, Pearl LH. An iron-sulfur cluster in the family 4 uracil-DNA glycosylases. *J Biol Chem* 2002;277:16936–40.
- [21] Swan MK, Johnson RE, Prakash L, Prakash S, Aggarwal AK. Structural basis of high-fidelity DNA synthesis by yeast DNA polymerase delta. *Nat Struct Mol Biol* 2009;16:979–86.
- [22] Lippi M, Passerini A, Punta M, Rost B, Frasconi P. MetalDetector: a Web server for predicting metal-binding sites and disulfide bridges in proteins from sequence. *Bioinformatics* 2008;24:2094–5.
- [23] Brzoska K, Meczynska S, Kruszewski M. Iron-sulfur cluster proteins: electron transfer and beyond. *Acta Biochim Pol* 2006;53:685–91.

Fig. 3. A cysteine-rich insertion in Pol2. (a) Schematic of the exo-pol module in the catalytic subunit of eukaryotic B-family polymerases. The catalytic core consists of the N-terminal, palm, fingers, and thumb domains for polymerase activity; and an exonuclease domain for proofreading activity. Approximate location of conserved motifs A and B in the palm and fingers domains, respectively, is indicated. A cysteine-rich insertion (Pol2^{ins}) is present between motifs A and B of Pol2 (yellow) but not within Pol1, Pol3, and Rev3. (b) Sequence alignment of the region between motif A and motif B for *S. cerevisiae* Pol1, Pol3, and Rev3 with Pol2 orthologs. *Sc*, *S. cerevisiae*; *Dr*, *Danio rerio*; *Mm*, *Mus musculus*; *Hs*, *Homo sapiens*. For clarity, only regions between motifs A and B are shown. Palm domain amino acids are highlighted in cyan; Pol2^{ins} residues, in yellow; and the fingers domain, in wheat. Cysteines mutated to serine in this study and conserved in Pol2 orthologs are highlighted in red boxes. Other semi-conserved cysteines are highlighted in gray. Amino acid sequences of Pol2 and homologs were aligned using the program PROMALS3D, and the alignments were visualized and formatted with JalView. (c) Model of Pol2 Δ CTD generated by using the structure of Pol3 Δ CTD (PDB ID 3IAY) as template [21]. Palm and fingers domain are shown in cyan and wheat, respectively. Approximate location Pol2^{ins} in the hinge region between the palm and fingers domains is shown by a yellow oval. (d) Pol2 Δ CTD^{mut} (C665S, C668S, and C677S) lacking the Fe-S cluster is deficient in DNA synthesis. Lane 1: DNA template-primer substrate only. DNA synthesis activity of Pol2 Δ CTD (lanes 2–4) and Pol2 Δ CTD^{mut} (lanes 5–7) in the presence of all four dNTPs. Exonuclease activity of Pol2 Δ CTD (lanes 8–10) and Pol2 Δ CTD^{mut} (lanes 11–13), respectively. The DNA polymerase assay (5 μ l) contained 25 mM Tris-HCl (pH 7.5), 10% glycerol, 1 mM DTT, 0.1 mg/ml bovine serum albumin, 10 nM DNA substrate, and 10 μ M each of dGTP, dATP, dTTP, and dCTP. Reactions were initiated by the addition of various concentrations of DNA polymerase and were carried out for 10 min at 30 °C. Reactions were terminated by the addition of 30 μ l of 95% formamide containing 0.03% each of bromophenol blue and xylene cyanol. Reaction products were denatured by heating to 95 °C for 3 min and resolved by separation on 12% polyacrylamide gels containing 8 M urea. Gels were dried and reaction products were visualized and quantified on a Storm 860 phosphorimager (Molecular Dynamics) and IQTL (version 8.0; GE Life Sciences) software.

- [24] Johnson DC, Dean DR, Smith AD, Johnson MK. Structure, function, and formation of biological iron-sulfur clusters. *Annu Rev Biochem* 2005;74:247–81.
- [25] Klinge S, Nunez-Ramirez R, Llorca O, Pellegrini L. 3D architecture of DNA Pol alpha reveals the functional core of multi-subunit replicative polymerases. *EMBO J* 2009;28:1978–87.
- [26] Lill R, Muhlenhoff U. Maturation of iron-sulfur proteins in eukaryotes: mechanisms, connected processes, and diseases. *Annu Rev Biochem* 2008;77:669–700.
- [27] Stehling O, Vashisht AA, Mascarenhas J, Jonsson ZO, Sharma T, Netz DJ, et al. MMS19 assembles iron-sulfur proteins required for DNA metabolism and genomic integrity. *Science* 2012;337:195–9.
- [28] Gari K, Leon Ortiz AM, Borel V, Flynn H, Skehel JM, Boulton SJ. MMS19 links cytoplasmic iron-sulfur cluster assembly to DNA metabolism. *Science* 2012;337:243–5.
- [29] Veatch JR, McMurray MA, Nelson ZW, Gottschling DE. Mitochondrial dysfunction leads to nuclear genome instability via an iron-sulfur cluster defect. *Cell* 2009;137:1247–58.
- [30] Pursell ZF, Kunkel TA. DNA polymerase epsilon: a polymerase of unusual size (and complexity). *Prog Nucleic Acid Res Mol Biol* 2008;82:101–45.